



**INTERNATIONAL JOURNAL OF ENGINEERING SCIENCES & RESEARCH
TECHNOLOGY**

**AN APPLICATION OF ASYMMETRICAL GLASS FIBRE-REINFORCED PLASTICS
FOR THE MANUFACTURE OF CURVED FIBRE REINFORCED CONCRETE**

Henrik L. Funke*, Sandra Gelbrich, Lars Ulke-Winter, Lothar Kroll, Carolin Petzoldt

* Institute of Lightweight Structures, Technische Universität Chemnitz, Chemnitz, Germany

Institute of Lightweight Structures, Technische Universität Chemnitz, Chemnitz, Germany

Institute of Lightweight Structures, Technische Universität Chemnitz, Chemnitz, Germany

Institute of Lightweight Structures, Technische Universität Chemnitz, Chemnitz, Germany

Institute of Lightweight Structures, Technische Universität Chemnitz, Chemnitz, Germany

ABSTRACT

There was developed a novel technological and constructive approach for the low-cost production of curved freeform formworks, which allow the production of single and double-curved fibre reinforced concrete. The scheduled approach was based on a flexible, asymmetrical multi-layered formwork system, which consists of glass-fibre reinforced plastic (GFRP). By using of the unusual anisotropic structural behavior, these GFRP formwork elements permitted a specific adjustment of defined curvature. The system design of the developed GFRP formwork was examined exhaustively. There were designed, numerically computed and produced prototypical curved freeform surfaces with different curvature radii.

The fibre reinforced concrete had a compressive strength of 101.4 MPa and a 3-point bending tensile strength of 17.41 MPa. Beyond that, it was ensured that the TRC had a high durability, which has been shown by the capillary suction of de-icing solution and freeze thaw test with a total amount of scaled material of 874 g/m² and a relative dynamic E-Modulus of 100% after 28 freeze-thaw cycles.

KEYWORDS: fibre reinforced concrete, asymmetrical glass fibre-reinforced plastics, curved concrete, high performance concrete.

INTRODUCTION

Apart from designing claddings, the focus in civil engineering increasingly moves to sustainability and resource efficiency, because future-oriented living and building is hardly viable without a significant increase of resource efficiency. With respect to resource efficiency, optimized building with low input (material, energy, area) during the complete lifecycle of a building means to meet the requirements of the residents regarding indoor environment quality and home comforts.

Using the material and technologies that are currently available, the practical implementation of these requirements rather expensive and therefore reaches its limits easily. The application of new high-performance materials which are inorganic-non-metallic offers more freedom for construction. Fiber-reinforced concrete facilitates the production of thin-walled, single- and double-curved free-form elements which are highly suitable for lightweight construction and comply with design requirements regarding surface quality /1-3/. Another advantage in comparison to ordinary reinforced concrete is that

corrosion can be largely excluded. In this way, filigree constructions of minimal thickness can be realized /4-5/.

A crucial technological objective of fibre reinforced concrete elements is the development of complex solid preform-structures. These are produced by processing flat structures through appropriate cutting /6/. The soft-elastic behavior of the 3D-textiles can be influenced to a large extent by modifying parameters such as stiffness, alignment and concentration of pile threads. In this way, it can be adjusted to the defined curvature. Although selectively deformable textile 3D-structures, for instance spacer fabric, for the reinforcement of concrete lightweight elements exist, the corresponding formwork elements are only in an early stage of development. These elements are essential for the realization of concrete shell structures that can be curved in any way.

Currently, the only possible shapes of shell structures are that of domes, hyperbolic paraboloids and conoids. Their production furthermore entails a considerable amount of material and high costs /7-8/. Also the mathematical description of the predetermined

complex freeform surfaces and the anisotropic material characteristic is difficult /9-10/. In the field of computer-aided visualization, different methods have been developed for the shape optimization of surfaces and their static construction calculation and design. However, these technologies are until now not applied in formwork production /11/. Among the common formwork techniques are conventionally segmented steel and wood systems, pneumatically supported and modeled formworks and combinations of them /12-13/.

This paper presents the results of tests carried out on asymmetrical glass fibre-reinforced plastics for the manufacture of curved fibre reinforced. The focus of this research work is on the numerical calculation and experimental verification of flexible, asymmetrical GFRP formworks and the production of curved fibre reinforced concrete-elements. Thus, the development of a suitable fibre reinforced concrete plays an important part of this paper, which includes the testing of mechanical properties and durability aspects of the fiber-reinforced concrete.

MATERIAL AND METHODS

Components of fibre reinforced concrete

The development of the fine grained concrete was focused on the workability of the fresh concrete as well as the durability and a good bonding between concrete matrix and fibre reinforcement. Table 1 shows the qualitative and quantitative composition of the fine grained concrete mix. In addition to ordinary white Portland cement CEM I 52.5 R (EN 197-1), a high content of an amorphous aluminosilicate as a pozzolana was used (Table 1). The high content of this pozzolana (22 mass percent of cement) results in a higher durability and enhanced bond between the glass fibres and concrete matrix in comparison to pure ordinary Portland cement. Dolomite sand with a grain size of 0 to 1 mm and dolomite powder with an average grain size of 70 μm were used as aggregate and filler. The short alkali-resistant (AR) glass-fibres (16 mass percent of ZrO_2) was 12 mm long and had a length weight of 45 g/kmA super plasticizer based on polycarboxylate ether (PCE) was used with a PCE solid content of 30 mass percent. The water binder ratio was 0.38.

Table 1: Qualitative and quantitative composition of the fine grained concrete mix

Component	Content in kg/m ³	Mass fraction in %
White cement CEM I 52.5 R	550	22,99
Amorphous aluminosilicate	120	5,02
Dolomite sand 0,5/1,0 ($x_{50} = 0,71$ mm)	1280	53,51
Dolomite filler ($x_{50} = 70$ μm)	160	6,69
Water	255	10,66
AR-glass fibres (12 mm, integral)	19	0,79
superplasticizer	8	0,33

The fine grained concrete was mixed with the intensive mixer Eirich R05T. The mixing parameters are shown in Table 2. The mixing time was 5 min in total. The fresh concrete was tested according to DIN

EN 12350. Air content and bulk density of the fresh concrete were determined by means of an air content testing device, following DIN 18555-2.

Table 2: Mixing parameters for the production of fine concrete

	component	mixing principle	mixing power in %	mixing time in s
1.	binders + aggregates	counter rotation	15	60
2.	75 % of water	co-rotation	50	90
3.	super plasticizer	co-rotation	50	60

4.	residual water	co-rotation	50	30
5.	ar-glass fibres	co-rotation	60	60

Determination of the hardened concrete characteristics

The samples for the tests to be performed on the hardened concrete were stored dry, according to DIN EN 12390-2. The compressive strength was determined by means of the Toni Technik ToniNorm (load frame 3000 kN) following DIN EN 12390-3, with cubes having an

edge length of 150 mm (Figure 1a). The pre-load was 18 kN. The 3-point bending tensile strength (Figure 1b) was determined with samples which measured 225 x 50 x 15 mm³ (length x width x height), based on DIN EN 12390-5 and ToniNorm (test frame 20 kN). The span width set was 200 mm and the load speed 100 N/s constant.



(a) compressive strength



(b) 3-point bending tensile strength

Figure 1: Determination of compressive strength and 3-point bending tensile strength
 To validate the durability of the fibre reinforced concrete, the capillary suction of de-icing solution and

freeze thaw test (CDF-test) was measured by the Schleibinger Freeze-Thaw-Tester (Figure 2) with standard agent solution according to the recommendations of RILEM TC 117-FDC.



Figure 2: Determination of the capillary suction of de-icing solution and freeze thaw test

Components for Glass-Fibre Reinforced Plastic

An unidirectional (UD) reinforced fabric UT-E500 by GURIT Holding AG was used for the production of the asymmetrical GFRP formwork. The UT-E500 consisted of an alumino-borosilicate glass and had an area density of 500 g/sqm. For the thermosetting resin matrix, the epoxy resin Epilox® T19-27 by LEUNA-Harze GmbH was used. By means of manual laminating, UD single layers were made from the UD

fabric and the epoxy resin. They had a fibre volume content of almost 30%. Within this UD single layer, the independent parameters: longitudinal (E1) and transverse (E2) moduli of elasticity, Poisson's ratio ν_{12} , shear modulus G12 and the coefficients of linear thermal expansion α_1 and α_2 between +20 and +120 °C were determined experimentally. Table 1 shows the results of these tests.

Table 3: Parameters of the unidirectional single layer

E ₁	E ₂	ν_{12}	G ₁₂	$\alpha_{1(20/120)}$	$\alpha_{2(20/120)}$
GPa	GPa	-	GPa	10 ⁻⁶ ·K ⁻¹	10 ⁻⁶ ·K ⁻¹
23.7	6.4	0.3	1.6	7	130

Adjustment and determination of defined curvatures

The determined basic parameters of the unidirectional single layer (Table 3) were used for the analytical and numerical calculation of multi-layered formworks,

which showed both a balanced symmetrical and an asymmetrical construction. The GFRP formwork with a plate size of 50 x 50 cm² was made of 11 UD single layers with total thickness of 3.3 mm (Figure 3).

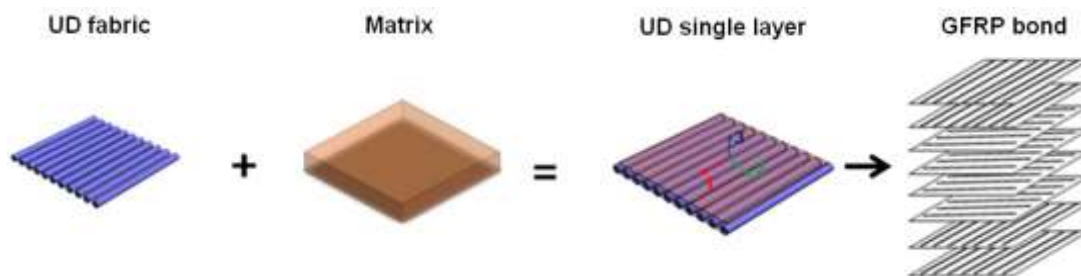


Figure 3: Process chain of anisotropic GFRP layered bond structures

After the production of the GFRP bond, the thermosetting matrix was cured in a heating cabinet over a period of 6 hours at a constant temperature of 120 °C. After curing, the GFRP bond were cooled to room temperature (20 °C). Due to this difference in

temperature of -100 K, residual stress caused a small curvature of the anisotropic layer structure. Afterwards, high curvatures were caused by external preloading (up to a material load of R= 0.95 after CUNTZE criterion), utilizing the coupling effects that

result from the GFRP bond (Figure 4).

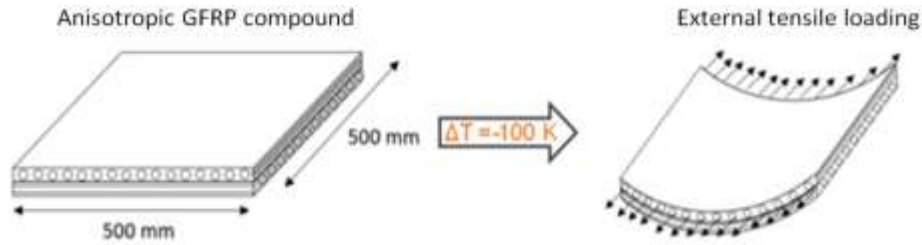


Figure 4: Temperature and tensile load of anisotropic GFRP layered bond structures for the adjustment of curvature states

The calculations of the coupling effects caused by anisotropy were conducted analytically with the Classical Laminate Theory (CLT) and the First Order Shear Deformation Theory (FSDT). For the experimental verification of the anisotropic coupling

effects calculated beforehand, selected GFRP bonds segments were produced and tested in the institute's own structural test bench with the ABD-testing device (Figure 5).

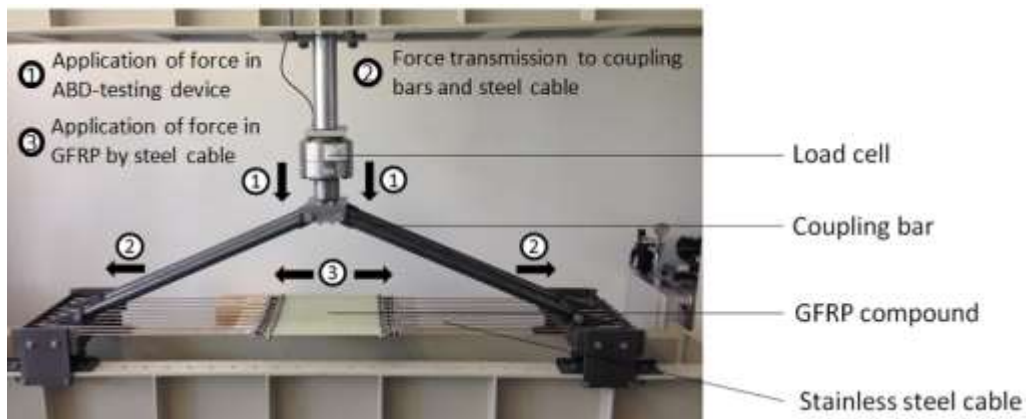


Figure 5: ABD-testing device

The results were used during the further procedure for the determination of the functional relations of curvatures, process parameters and geometrical parameters. Based on that, the analysis and identification of single and double curved basic forms

was conducted. Their combination resulted in a maximum of defined freeform surfaces. The experimental analysis of the curves was conducted with the aid of the optical forming-analysis-systems ARGUS and ARAMIS by GOM (Figure 6).

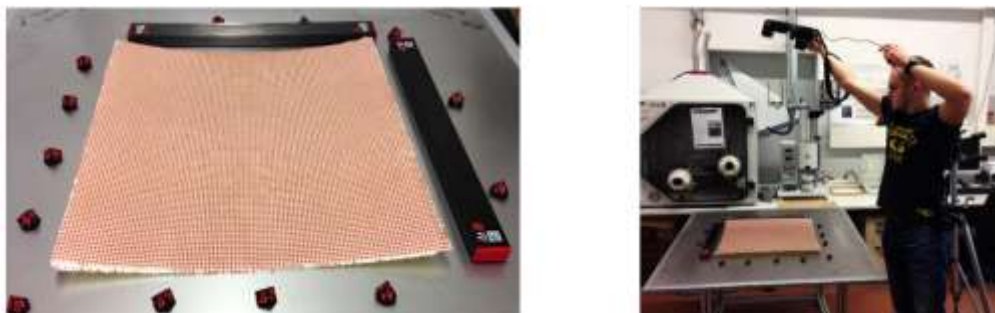


Figure 6: Curved GFRP layered bond structure plate with coded reference mark (picture on the left) and test set-up of the optical forming-analysis-system ARGUS (picture on the right)

RESULTS AND DISCUSSION

Properties of fresh and hardened concrete

Table 4 shows the fresh and hardened concrete characteristics after 28 days. With a high flow capacity (diameter of the resulting flow table test: 400 mm) the fresh concrete complies with the flow class F2 according to DIN EN 206-1. The air content tester showed an air volume content of 4.5% and a geometric bulk density of 2.32 g/cm³ in the fresh concrete. The 3-point bending tensile strength was 17.41 MPa after 28 days.

The total shrinkage deformation, determined with a

shrinkage channel, was 0.72 mm/m. The reasons for this were first the high binder content, and the high chemical shrinkage resulting from that. Second, autogenously shrinkage increased due to the low water-binder ratio. Drying shrinkage could be practically eliminated due to a two days aftertreatment including humidifying and protection against draft. The high total shrinkage deformation did not lead to shrinkage cracking and was therefore not harmful. The fine grained concrete showed a high durability, which was validated in the CDF-Test ($m_{28} = 874 \text{ g/m}^2$ and $R_{u,28} = 100\%$) after 28 freeze-thaw cycles.

Table 4: Properties of fresh and hardened fibre reinforced concrete

characteristic	fresh concrete	hardened concrete
geometric bulk density	2.32 g/cm ³	2.25 g/cm ³
flow spread	400 mm	-
air content	4.5 Vol.-%	-
linear shrinkage	0.72 mm/m	
compressive strength	-	101.4 MPa
3-point bending tensile strength	-	17.41 MPa
CDF	$m_{28} = 874 \text{ g/m}^2$ $R_{u,28} = 100\%$	

Figure 7 shows the compressive strength development of the hardened fine grained concrete. Over 90 percent of the 28-day strength (101.4 MPa) is already reached after seven days. Thus, it can be concluded that the hydration of the C-S-H- and C-A-H-phases is almost

complete. The nearly completed C-S-H- and C-A-H-phase formation, which is the practical end of the chemical and autogenous shrinkage, can be observed by the decrease in shrinkage deformation after seven days (0.65 mm/m).

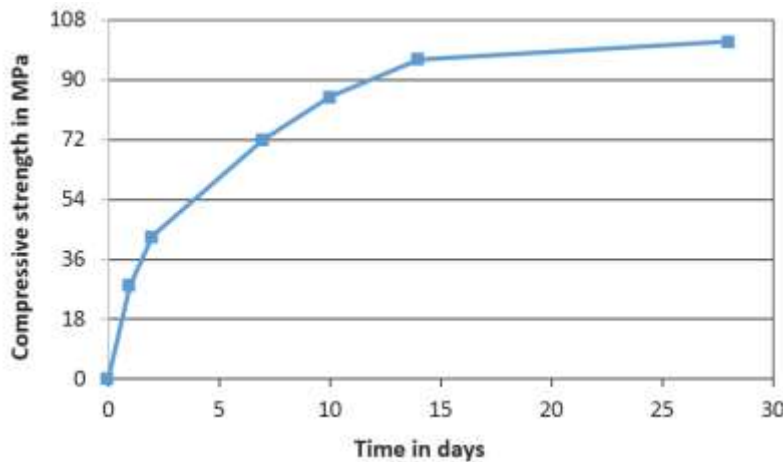


Figure 7: Development of the compressive strength of the fibre reinforced concrete

Theoretical and experimental verification of major curves

The theoretical major curves (for calculation approach cf. /Kroll, 2005/) of an asymmetrical layer structure with 0°- and 90°-layer content (90n/0m) are

exemplarily depicted for two loading cases in Figure 8, dependent on the 0°-layer content. The curves increased with increasing layer content accompanied by increasing anisotropy, both in the 1- and in the 2-axis (Figure 8).

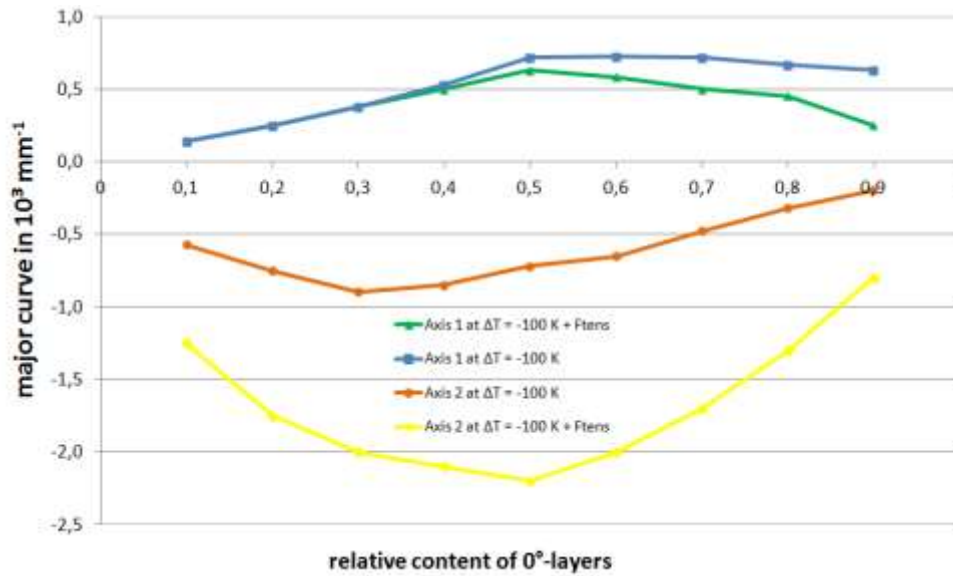


Figure 8: Theoretical major curve of an asymmetrical layer structure (90_n/0_m), depending on the portion of 0°-layer, with pure temperature load ($\Delta T = -100\text{ K}$) and superimposed temperature and tensile load

The highest anisotropy was found with a relative 0°-layer content of about 50 percent. This caused the largest curvature around both axes (Figure 8 and 9). A further increase of the 0°-layer content caused a decrease of curvature, because the anisotropy of the

GFRP layered bond structure decreased. Due to external preload forces, the tensile load caused an increase of curvature around the 2-axis. At the same time, curvature around the 1-axis decreased, due to traction.

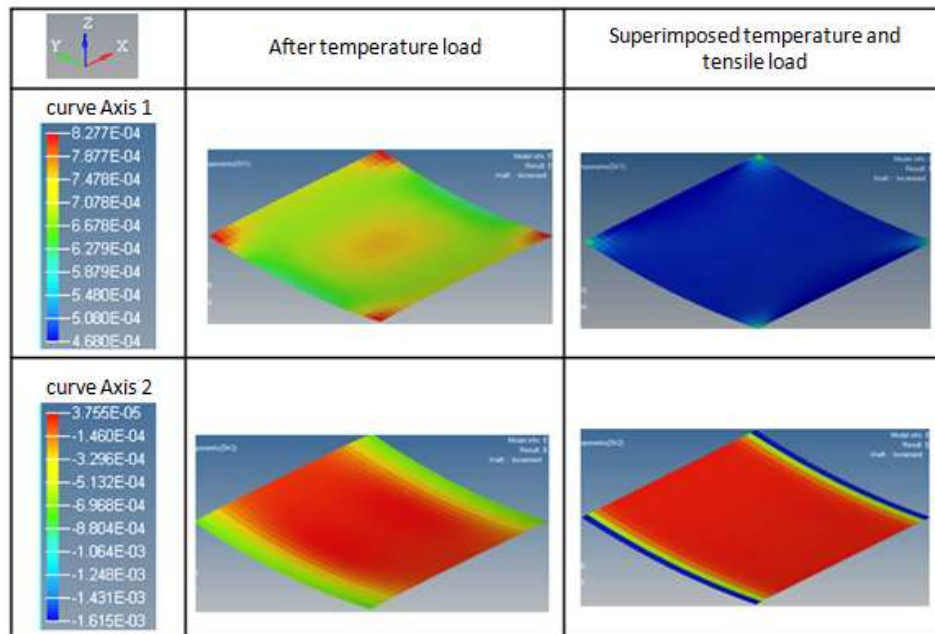


Figure 9. Theoretical major curve of the asymmetrical layer structure 90_n/0_m depending on the portion of 0°-layer, with pure temperature load ($\Delta T = -100\text{ K}$) and superimposed temperature and tensile load

Figure 10 displays the theoretical and experimentally verified major curves of the asymmetrical layer structure (90_n/0_m), depending on 0°-layer content

with a pure temperature load of ($\Delta T = -100\text{ K}$). The major curves around the 1-axis that were determined experimentally agreed qualitatively and

approximately also quantitatively with the major curve that was calculated previously (Figure 10). The minor quantitative differences between the calculated and the experimentally verified major curves around the 1-axis were caused by physico-chemical reactions of the thermosetting matrices. In the calculations, these

matrices could be included only insufficiently. Apart from chemical shrinkage, they included residual stress caused by swelling after increased water absorption in or among the molecular chains of the thermosetting matrices (Schürmann, 2007).

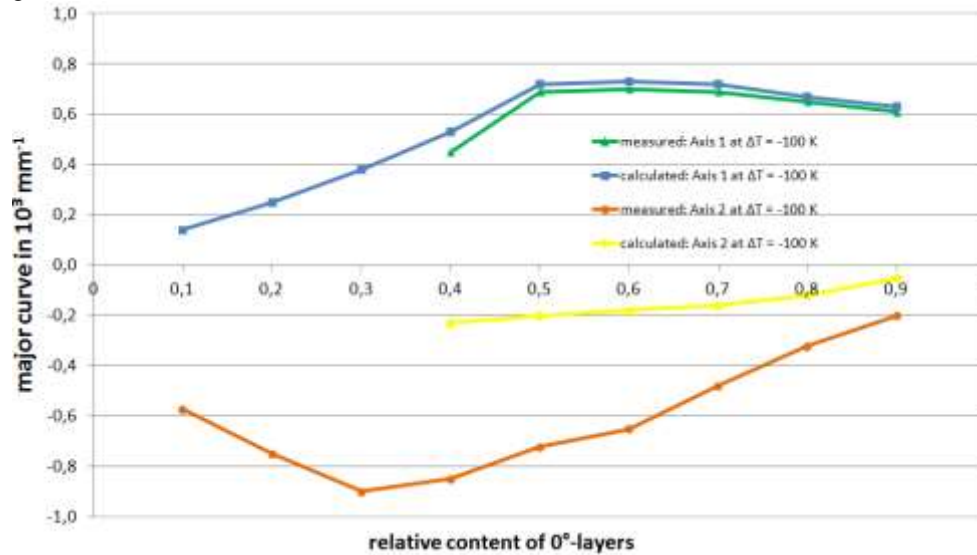


Figure 10. Comparison between calculated and experimentally verified major curvatures at ΔT = -100 K

In contrast to that, there are greater differences between the calculated and experimentally verified major curves around the 2-axis. In reality however, only one of the major curves prevails, due to stability problems (problems with the transmission/distribution of forces). In this case, this is the curvature around the 1-axis.

Production Tests of Concrete Lightweight Element

Of special importance during the production tests was to ensure the evenness of the concrete layer thickness, consistently good surface quality, sufficient stability of the GFRP formwork and to avoid critical cracks both in the concrete and in the formwork system. Also essential were good sheeting qualities (Figure 11).



(a) Demonstrator (surface area: about 5.5 square meter)



(b) Research pavilion (based on 4 demonstrators)

Figure 11: Production tests of concrete fibre reinforced concrete elements

CONCLUSIONS

The aim of this research project was to develop a flexible, multi-layered formwork system made from

glass-fibre reinforced plastic, which allows for a specific adjustment of defined curvature states, utilizing the structural behavior influenced by anisotropy. The adjustment of the coupling effects,

which are induced by anisotropy, were calculated in advance analytically by means of the extended laminate theory and numerically by means of the Finite Element Method. A good correspondence of the respective results for the representative shell structures was proven. An experimental verification of these intrinsic coupling phenomena has been conducted with specifically produced textile reinforced concrete-lightweight-elements. Based on the yielded results, ideal layer constructions for the key curvature states and their variation range could be set. Beyond the efficient production of curved concrete-lightweight-elements, GFRP formworks employ excellent concrete qualities on highest classes of face concrete. This contributes to the generation of new forms of architecture and buildings. The intensively conducted numerical, technological and experimental tests show that combinations of concrete and stabilizing spacer fabrics permit the implementation of single and double curved, multi-axially loaded surface structures. Furthermore, the flexible GFRP formwork design allows not only a location-independent implementation of freeform surfaces following the principle “form follows form” but also results in thin-walled and thus extremely light concrete shell structures.

ACKNOWLEDGEMENTS

This work was supported by the Priority Program SPP 1542 of the German Research Foundation (DFG) and the Federal Cluster of Excellence EXC 1075 “MERGE Technologies for Multifunctional Lightweight Structures”. The authors would like to acknowledge with gratitude the foundation’s financial support.

REFERENCES

1. Brameshuber W. Textile Reinforced Concrete, RILEM Report 36. State-of-the-Art Report of RILEM Technical Committee, TC 201-TRC, 2006.
2. Mumanya S, Tait R and Alexander M. Mechanical behaviour of Textile Concrete under accelerated ageing conditions, *Cement & Concrete Composites*, 32, 580–588, 2012.
3. Greiner, S. (2007). Zum Tragverhalten von Schalen aus ultrahochfestem Faserfeinkornbeton (UHFFB). *Z. Beton- und Stahlbetonbau*, 100(9), 77-80.
4. Curbach, M., & Jesse, F. (2010). Verstärken mit Textilbeton. In K. Bergmeister, F. Fingerloos, & J.-D. Wörner (Eds.), *Betonkalender 2010, Teil 1, Abschn. VII*. Berlin: Ernst & Sohn.
5. Curbach, M., & Scheerer, S. (2011). Concrete light – Possibilities and Visions. In V. Šrůma (Ed.), *Proceedings of the fib Symposium Prague 2011: Concrete Engineering for Excellence and Efficiency* (pp. 29-44). 8.-10. June, DVD-ROM.
6. Curbach, M., Ortlepp, S., Brückner, A., Kratz, M., Offermann, P., & Engler, T. (2003). Entwicklung einer großformatigen, dünnwandigen, textildbewehrten Fassadenplatte. *Z. Beton- und Stahlbetonbau*, 98(6), 345-350.
7. Hofstadler, C. (2008). *Scholarbeiten*. Berlin, Heidelberg: Springer-Verlag
8. Herzog, T., & Moro, J. L. (1992). Gespräch mit Felix Candela. In *Arcus 18: Zum Werk von Felix Candela – Die Kunst der leichten Schalen* (pp. 10-22). Köln: Verlagsgesellschaft Rudolph Müller
9. Kaufmann, J. (2014). Beitrag zu anisotropiebedingten Koppelleffekten bei rotationssymmetrischen mehrschichtigen Faserverbundbauteilen. Promotionsschrift, TU Chemnitz.
10. Kroll, L. (2005). Berechnung und technische Nutzung von anisotropiebedingten Werkstoff- und Struktureffekten für multifunktionale Leichtbauanwendungen. Habilitationsschrift, TU Dresden.
11. Dallinger, S., Pardatscher, H., & Kollegger, J. (2009). Zweifach gekrümmte Schalen aus Betonfertigteilen. *Z. Forschung & Entwicklung für Zement und Beton*, 5, 32-33.
12. DE 3841579 A1: Schalung für großformatige gekrümmte Stahlbetonfertigteile, Werner Zapf KG. Zapf, W., 1990
13. EP 0 238 168 A1: Verfahren und Vorrichtung zum Formen von gebogenen Sektionen aus Beton, Henri, V., 1987